



Arterial spin labeling imaging for the detection of cerebral blood flow asymmetry in patients with corticobasal syndrome

Tomohisa Yamaguchi¹ · Masamichi Ikawa^{1,2,3} · Souichi Enomoto¹ · Norimichi Shirafuji¹ · Osamu Yamamura¹ · Tetsuya Tsujikawa² · Hidehiko Okazawa² · Hirohiko Kimura⁴ · Yasunari Nakamoto¹ · Tadanori Hamano^{1,5}

Received: 21 February 2022 / Accepted: 1 April 2022 / Published online: 11 April 2022
© The Author(s), under exclusive licence to Springer-Verlag GmbH Germany, part of Springer Nature 2022

Abstract

Purpose Corticobasal syndrome (CBS) and Parkinson's disease (PD) both present with asymmetrical extrapyramidal symptoms, often leading to a diagnostic dilemma. Patients with CBS frequently show cerebral blood flow (CBF) asymmetry alongside asymmetrical cortical atrophy. This study aimed to evaluate the clinical utility of arterial spin labeling (ASL) magnetic resonance imaging (MRI) to detect CBF asymmetry in patients with CBS.

Methods We retrospectively investigated asymmetries of regional CBF and cortical volume, measured using ASL and T1-weighted MRI, in 13 patients with CBS and 22 age-matched patients with PD. Regional CBF and cortical volume values were derived from nine brain regions on each side. CBF and volume asymmetries were calculated as %difference in each region, respectively.

Results CBF asymmetry showed significantly greater differences in seven of nine regions, such as the perirolandic area (−8.7% vs. −1.4%, $p < 0.001$) and parietal cortex (−9.7% vs. −1.3%, $p < 0.001$) in patients with CBS compared with patients with PD. In contrast, significant differences in volume asymmetry were observed in three regions included within the seven regions showing CBF asymmetry, which indicated that CBF asymmetry has greater sensitivity than volume asymmetry to detect asymmetry in CBS.

Conclusion ASL imaging showed significant CBF asymmetry in a wider range of brain regions in patients with CBS, which suggests that noninvasive MRI with ASL imaging is a promising tool for the diagnosis of CBS, with advantages that include the simultaneous evaluation of asymmetrical hypoperfusion in addition to focal atrophy.

Keywords Arterial spin labeling · Asymmetry · Cerebral blood flow · Corticobasal syndrome · Parkinson's disease

Introduction

Corticobasal syndrome (CBS) is a clinical diagnostic entity characterized by asymmetrical symptoms due to basal-ganglionic and cerebral cortical dysfunction, such as akinesia, rigidity, and apraxia [1]. Corticobasal degeneration (CBD) is the dominant pathological etiology of CBS; however, various neurodegenerative pathologies, such as progressive supranuclear palsy, Alzheimer's disease, and frontotemporal lobar degeneration, are also responsible for CBS [2, 3].

Several clinical criteria for CBS have been proposed [1–3], all of which indicate that an asymmetrical presentation of extrapyramidal symptoms is a key component of the criteria [4]. Similarly, most patients with Parkinson's disease (PD) also present with asymmetrical extrapyramidal symptoms [5]. Although the causal mechanism for asymmetrical manifestations remains unclear in both CBS and

✉ Masamichi Ikawa
iqw@u-fukui.ac.jp

¹ Second Department of Internal Medicine, Faculty of Medical Sciences, University of Fukui, 23-3 Matsuoka-Shimoaizuki, Eiheiji, Fukui 910-1193, Japan

² Biomedical Imaging Research Center, University of Fukui, 23-3 Matsuoka-Shimoaizuki, Eiheiji, Fukui 910-1193, Japan

³ Department of Advanced Medicine for Community Healthcare, Faculty of Medical Sciences, University of Fukui, 23-3 Matsuoka-Shimoaizuki, Eiheiji, Fukui 910-1193, Japan

⁴ Department of Radiology, Faculty of Medical Sciences, University of Fukui, 23-3 Matsuoka-Shimoaizuki, Eiheiji, Fukui 910-1193, Japan

⁵ Department of Aging and Dementia (DAD), Faculty of Medical Sciences, University of Fukui, 23-3 Matsuoka-Shimoaizuki, Eiheiji, Fukui 910-1193, Japan

PD, the involvement of genetic and environmental factors has been assumed in PD [6], which may be extrapolated to CBS. Because of asymmetrical extrapyramidal symptoms observed in both CBS and PD, it is sometimes challenging to distinguish between these diseases, especially in the early disease phase.

Along with clinical findings, asymmetrical morphological changes (i.e., atrophy) on brain magnetic resonance imaging (MRI) aids in the diagnosis of CBS. Brain MRI usually shows asymmetrical partial atrophy in the hemisphere contralateral to the more clinically affected side in patients with CBS [7–9]; however, assessment of asymmetrical atrophy is occasionally inconsistent. Single-photon emission computed tomography (SPECT) using perfusion imaging radioligands, such as *N*-isopropyl-(^{123}I)-*p*-iodoamphetamine (^{123}I -IMP) and $^{99\text{m}}\text{Tc}$ -hexamethylpropyleneamine oxime ($^{99\text{m}}\text{Tc}$ -HMPAO), and positron emission tomography (PET) with ^{18}F -fluorodeoxyglucose (^{18}F -FDG), has shown an asymmetrical decrease in the cerebral blood flow (CBF) [9–13] or glucose metabolism [9, 14–16] in patients with CBS. Since these asymmetrical findings are unique to CBS [9, 12, 13, 17, 18], simultaneous imaging evaluation of regional CBF asymmetry in addition to asymmetrical atrophy could be useful in diagnosing CBS, especially when differentially diagnosing CBS from PD. However, the application of radionuclide imaging has many limitations in clinical settings, such as the need for a radiopharmaceutical injection, radiation exposure, and the relatively higher cost and longer scan time.

Arterial spin labeling (ASL) imaging is a brain MRI sequence that produces perfusion images noninvasively through using magnetically labeled endogenous blood, via a simple subtraction of labeled and control images [19, 20]. This imaging procedure enables simultaneous acquisition of morphological and perfusion images in a single MR scan

and has many advantages, such as its short scanning time (<5 min) and no requirement for contrast media or radioligand injection. ASL imaging has been widely used to assess brain hemodynamic changes in cerebrovascular diseases and various neurodegenerative disorders such as PD [21], spinocerebellar degeneration [22], and mitochondrial disease [23]. While one case report showed an asymmetrical regional reduction in CBF corresponding to partial cortical atrophy on brain MRI with ASL imaging in a patient with CBS [24], whether ASL imaging can be used to identify the asymmetry of cerebral perfusion in patients with CBS remains unknown.

To evaluate the clinical utility of ASL imaging to detect CBF asymmetry in patients with CBS, we retrospectively investigated asymmetries of regional CBF and cortical volume measured using noninvasive MRI with ASL imaging in patients with CBS and compared the results with those in patients with PD.

Materials and methods

Patients

From June 2012 to June 2020, 13 consecutive patients with CBS (seven men and six women), aged 71.2 ± 8.4 years at the time of the MRI scan, who fulfilled the revised Cambridge criteria [4] were studied using brain MRI including ASL imaging, at the University of Fukui Hospital (Table 1). All patients with CBS presented with at least one of the following neurological manifestations: akinesia (observed in 100% of the patients), rigidity (92%), and apraxia (85%). Six (46%) patients had right-sided dominant symptoms. The mean Hoehn-Yahr stage was 1.6 ± 0.7 , and the mean disease duration was 3.3 ± 2.9 years. Eight (62%) patients were

Table 1 Demographic and clinical characteristics of patients with CBS and patients with PD

Patient group	CBS	PD	<i>p</i> value
<i>N</i>	13	22	
Age (mean \pm SD)	71.2 ± 8.4	69.0 ± 9.0	0.51
Sex (male/female)	7/6	11/11	1.00
Disease duration in years (mean \pm SD)	3.3 ± 2.9	3.0 ± 2.4	0.69
Dominancy of the symptoms (right/left)	6/7	13/9	0.50
Hoehn-Yahr stage (mean \pm SD)	1.6 ± 0.7	1.6 ± 0.8	0.75
Akinesia	13 (100%)	19 (86%)	0.27
Rigidity	12 (92%)	18 (82%)	0.63
Apraxia	11 (85%)	0 (0%)	<0.01
LEDD (mg)	223.1 ± 236.0	103.4 ± 181.3	0.16
PLD (1.5 s/2.0 s)	4/9	6/16	0.86

CBS, corticobasal syndrome; LEDD, levodopa equivalent daily dose; *N*, number of patients; PD, Parkinson's disease; PLD, post-labeling delay acquisitions for arterial spin labeling imaging; SD, standard deviation

being treated with antiparkinsonian therapy at the time of the MRI scan, and the mean levodopa equivalent daily dose (LEDD) was 223.1 ± 236.0 mg, calculated based on a review [25] (Supplementary Table 1).

We set up patients with PD as a control group since PD also presents with asymmetrical extrapyramidal symptoms similar to CBS, which often leads to misdiagnosis. Brain MRI data including ASL imaging obtained during the same period were leveraged in 22 age-matched patients with PD (11 men and 11 women; aged 69.0 ± 9.0 years at the time of the MRI scan), who fulfilled the UK brain bank criteria for a prospective diagnosis of PD [26] as a control (Table 1). Thirteen (59%) patients showed right-sided dominant symptoms. The mean Hoehn-Yahr stage was 1.6 ± 0.8 , and the mean disease duration was 3.0 ± 2.4 years. Ten (45%) patients were being treated with antiparkinsonian therapy at the time of the MRI scan, and the mean LEDD was 103.4 ± 181.3 mg (Supplementary Table 2).

No patients showed obvious stenosis or occlusion in the cerebral and carotid arteries on MR angiography. No prominent lesions, such as infarction, bleeding, or tumor, were observed on diffusion-weighted and fluid-attenuated inversion recovery (FLAIR) images. This retrospective case–control study was approved by the Research Ethics Committee of the University of Fukui (20,170,130) with a waiver of the need for the patients' informed consent.

Brain MRI

Brain MRI including T1-weighted and ASL perfusion sequences was performed using a 3 T-MR clinical scanner (Discovery MR750 3.0 T, GE Healthcare, Milwaukee, WI, USA) as a routine clinical scan. A high-resolution three-dimensional T1-weighted anatomical image was acquired using the following parameters: repetition time (TR) = 7.2 ms; echo time (TE) = 2.2 ms; inversion time (TI) = 700 ms; flip angle = 10; field-of-view (FOV) = 240 mm; 512×512 matrix; 224 slices; and voxel dimension = $0.47 \times 0.47 \times 0.7$ mm³.

To obtain a quantitative CBF image, a pseudo-continuous ASL scheme was employed [27]. A three-dimensional spiral fast spin-echo (FSE) sequence with background suppression covering the entire brain was obtained. The acquisition parameters were as follows: 7 arms with 512 points in each spiral arm, phase encoding in the *z*-direction = 34–40, section thickness = 4 mm, repetition time (TR) = 6 s, post-labeling delay (PLD) = 1.5 or 2.0 s, image reconstruction matrix = 128×128 , and number of excitations (NEX) = 3, as previously described [22, 23]. The numbers of patients who underwent ASL imaging with a PLD of 1.5 s comprised 4 (31%) and 6 (27%) in the CBS and PD groups, respectively (Table 1). To create a CBF image, an approximate proton density-weighted image was obtained using the same

acquisition parameters, with the exception of labeling at TR = 2 s and no background suppression. The T1 of arterial blood water and the blood/brain partition coefficient for the whole brain average were set to 1.6 s and 0.9, respectively.

Image processing

We performed image analysis using the PMOD software (version 3.6; PMOD Technologies Ltd., Zurich, Switzerland). The CBF image was co-registered to each patient's T1-weighted image. To create an individual anatomical parcellation of volumes of interest (VOIs), the N30R83 maximum probability atlas was adjusted to the T1-weighted image with a spatial normalization procedure using the PMOD software [28, 29]. A total of 86 regions were identified and converted to VOIs. To obtain a simplified VOI, we merged related VOIs into the following nine VOIs on each side (i.e., right and left): superior frontal, inferior frontal, perirolandic, medial temporal, temporal, parietal, and occipital cortices; lentiform nucleus; and cerebellar cortex (Fig. 1C). Regional CBF and cortical volume values were obtained by applying the VOIs to the CBF and T1-weighted images, respectively.

To compare CBF and cortical volume in nine brain regions between patients with CBS and patients with PD, we employed two analytical methods: (i) regional asymmetry and (ii) regional decrease. To evaluate the regional asymmetries of CBF and cortical volume, we defined the cerebral and cerebellar hemisphere contralateral to the more clinically affected side as the target hemisphere (TH), and the other hemisphere (i.e., the hemisphere ipsilateral to the more clinically affected side) as the rest hemisphere (RH). The asymmetries of CBF and volume values in each region were respectively calculated as %difference using the following equation: $(TH - RH) / RH \times 100$ (%). The raw values of CBF and volume derived from ASL and T1-weighted images were assigned in this equation. Separately, to assess the regional decreases in CBF and cortical volume, the regional raw values of CBF and volume were respectively normalized using the whole gray matter values in each patient. The normalized (i.e., percent to the whole gray matter values) CBF and volume values in each region belonging to the hemisphere contralateral to the more clinically affected side as the target hemisphere were calculated.

Statistical analysis

Data are presented as mean \pm standard deviation (SD). All statistical analyses were performed using SPSS statistics (version 23; IBM Corporation, Armonk, NY, USA) and R software (version 4.1.2; <http://www.R-project.org>), and $p < 0.05$ was considered statistically significant. Group differences were assessed using a two-tailed Mann–Whitney

U test. The Benjamini–Hochberg false discovery rate with a threshold *p* value of 0.05 was used to correct for region-wise multiple comparisons. Receiver operating characteristic (ROC) curves were plotted for each modality (i.e., CBF and volume) in each region to calculate the area under the curve (AUC) in distinguishing patients with CBS from patients with PD. DeLong’s test was employed to compare the ROC curves.

Results

Patient characteristics

No significant differences were found in terms of age, sex, disease duration, Hoehn-Yahr stage, and LEDD distribution between patients with CBS and those with PD (Table 1). Apraxia was more frequently observed in patients with CBS ($p < 0.01$), whereas most patients in both groups presented with akinesia and rigidity.

Representative cases

Figure 1 shows CBF images derived from ASL imaging and T1-weighted images of representative patients with CBS or PD.

Figure 1A shows brain MRI of the patient with CBS (Case 7, 72-year-old man) who had gradually developed akinesia of the left limbs and gait disturbance over a 3-year period. T1-weighted and CBF images showed asymmetrical atrophy and reduced CBF in the right frontoparietal cortex including the perirolandic area. CBF images also showed asymmetrical hypoperfusion in the right lentiform nucleus and the left cerebellum, although T1-weighted images showed no obvious atrophy in these regions. Cerebellar hypoperfusion may have been attributed to the crossed cerebellar diaschisis.

Figure 1B shows brain MRI of the patient with CBS (Case 5, 70-year-old man) who presented with a 3-year history of cheirospasm and dystonia of the right arm. T1-weighted images showed no obvious atrophy; however, CBF images showed asymmetrical hypoperfusion in the left superior frontal cortex and right cerebellum.

Figure 1C shows brain MRI of the patient with PD (Case 9, a 68-year-old woman) who presented with a 1-year history of right arm rigidity. Both CBF and T1-weighted images showed no obvious asymmetries.

In summary, CBF images showed asymmetrical hypoperfusion in the cortex as well as the contralateral cerebellum in patients with CBS (Fig. 1A, B). Asymmetrical decreased CBF was more distinct than cortical atrophy as observed on T1-weighted images, which suggests that cerebral

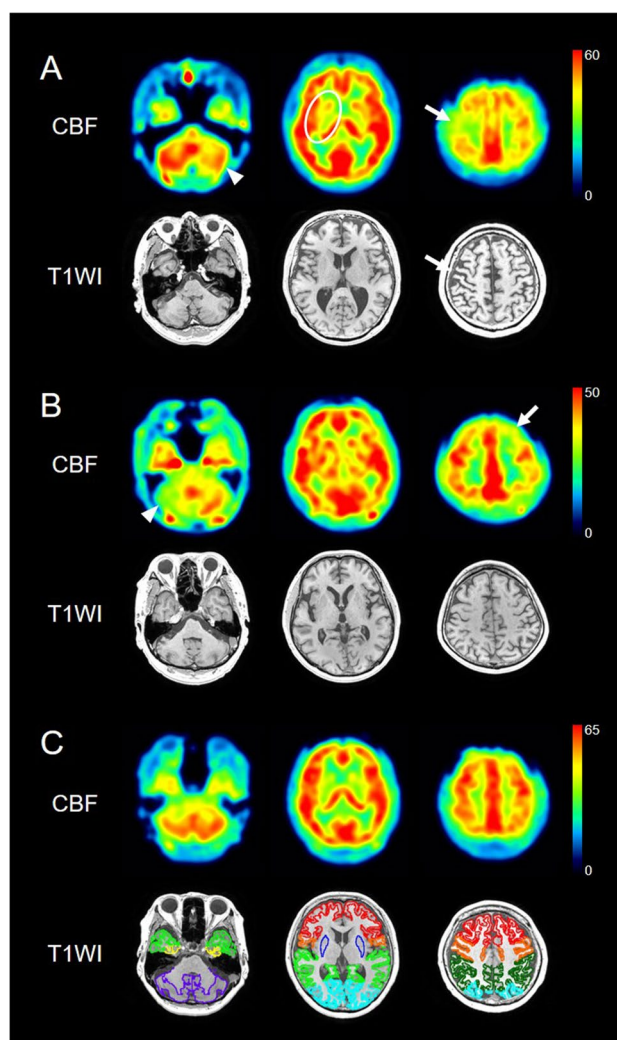


Fig. 1 Representative images of the cerebral blood flow (CBF) maps derived from arterial spin labeling (ASL) imaging with T1-weighted images (T1WIs) in patients with corticobasal syndrome (CBS) and in a patient with Parkinson’s disease (PD) **A** The patient with CBS (Case 7) showed asymmetrical atrophy and reduced CBF in the right frontoparietal cortex including the perirolandic area (arrows). Asymmetrical hypoperfusion was also observed in the right lentiform nucleus (circle) and the left cerebellum (arrowhead). **B** The patient with CBS (Case 5) showed asymmetrical hypoperfusion in the left superior frontal cortex (arrow) and right cerebellum (arrowhead). No obvious atrophy was observed in T1WIs. **C** The patient with PD (Case 9) showed no obvious asymmetries in both CBF and T1WIs. The color regions on the T1WIs show the volumes of interest: superior frontal (red), inferior frontal (not shown), perirolandic (orange), medial temporal (yellow), temporal (yellow-green), parietal (green), and occipital cortices (light blue); lentiform nucleus (blue) and cerebellar cortex (violet). The color bars indicate the range of CBF values (ml/100 mg/min).

hypoperfusion tends to be more extensively observed compared with cortical atrophy in patients with CBS. In contrast, both CBF and T1-weighted images showed no obvious asymmetries in a patient with PD (Fig. 1C).

Analyses of regional asymmetries of CBF and cortical volume

In the regional asymmetry evaluation, CBF asymmetry (%difference) differed significantly between patients with CBS and those with PD in the following seven of nine brain regions: perirolandic area (-8.7% vs. -1.4% , $p < 0.001$), parietal cortex (-9.7% vs. -1.3% , $p < 0.001$), occipital cortex (-7.7% vs. 0.7% , $p < 0.005$), cerebellar cortex (7.1% vs. -0.5% , $p < 0.005$), superior frontal cortex (-6.6% vs. -1.0% , $p < 0.005$), temporal cortex (-6.6% vs. -1.3% , $p < 0.01$), and lentiform nucleus (-5.1% vs. 0.7% , $p < 0.05$) (Fig. 2A). These findings showed asymmetrical hypoperfusion in these regions belonging to the hemisphere contralateral to the more clinically affected side except for the cerebellar cortex in patients with CBS. Interestingly, the cerebellar cortex showed a relative increase in CBF in the hemisphere contralateral to the more clinically affected side (Fig. 2A). This finding indicates a relative decrease in CBF in the cerebellar cortex ipsilateral to the affected side, which was probably caused by crossed cerebellar diaschisis.

Significant differences in cortical volume asymmetry (%difference) between patients with CBS and patients with PD were observed in the following three of nine brain regions: parietal cortex (-8.3% vs. -1.1% , $p < 0.001$), superior frontal cortex (-8.0% vs. -0.5% , $p < 0.001$), and perirolandic area (-11.2% vs. -0.2% , $p < 0.001$) (Fig. 2B), which indicated asymmetrical atrophy in these regions belonging to the hemisphere contralateral to the more clinically affected side in patients with CBS. These three regions were included within the regions showing significant CBF asymmetry.

The present study included two different post-labeling delay acquisitions, namely, 1.5 and 2.0 s for ASL imaging.

There was no significant difference ($p = 0.75$) in the mean CBF asymmetry values of the nine brain regions between patients with CBS in the 1.5 s group ($N = 4$, $-4.0 \pm 4.1\%$) and those in the 2.0 s group ($N = 9$, $-4.5 \pm 3.4\%$), which was comparable to the volume asymmetry in these patients ($-4.2 \pm 2.0\%$ vs. $-4.9 \pm 5.1\%$, $p = 0.75$).

ROC analysis of asymmetries in CBF and cortical volume

We further performed ROC analysis to distinguish the CBS group from the PD group for each of seven regions that showed a significant difference between patients with CBS and those with PD either in terms of CBF asymmetry or in cortical volume asymmetry (Fig. 3). The AUCs of CBF asymmetry showed good accuracy ($AUC > 0.7$) in all seven regions. In contrast, the AUCs of volume asymmetry showed good accuracy in only three regions. Although no significant differences in AUCs between CBF and volume asymmetries were observed in the seven regions, the AUCs of CBF asymmetry were greater than those of volume asymmetry in five regions.

Analyses of regional decreases in normalized CBF and cortical volume

To evaluate regional decreases in CBF and cortical volume, we compared the normalized CBF or cortical volume in nine brain regions belonging to the hemisphere contralateral to the more clinically affected side between patients with CBS and those with PD. The normalized CBF was significantly lower in the following two regions: perirolandic area (98.4% vs. 105.5% , $p < 0.001$) and parietal cortex (91.1% vs. 99.7% ,

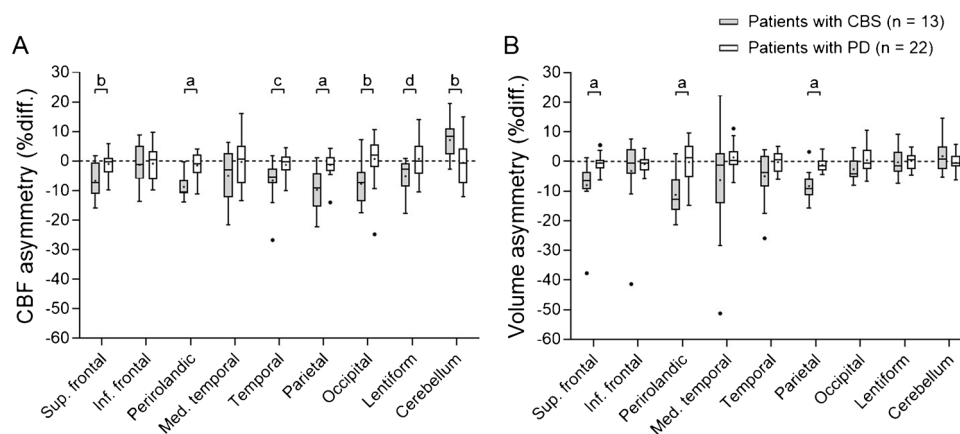


Fig. 2 Comparisons of cerebral blood flow (CBF) asymmetry and cortical volume asymmetry between patients with corticobasal syndrome (CBS) and patients with Parkinson's disease (PD) **A** CBF asymmetry (%difference) showed significant differences in seven of nine regions: superior frontal, perirolandic, temporal, parietal, and

occipital cortices; lentiform nucleus; and cerebellar cortex. **B** Volume asymmetry (%difference) showed significant differences in three of nine regions: superior frontal, perirolandic, and parietal cortices. p values: a < 0.001, b < 0.005, c < 0.01, d < 0.05

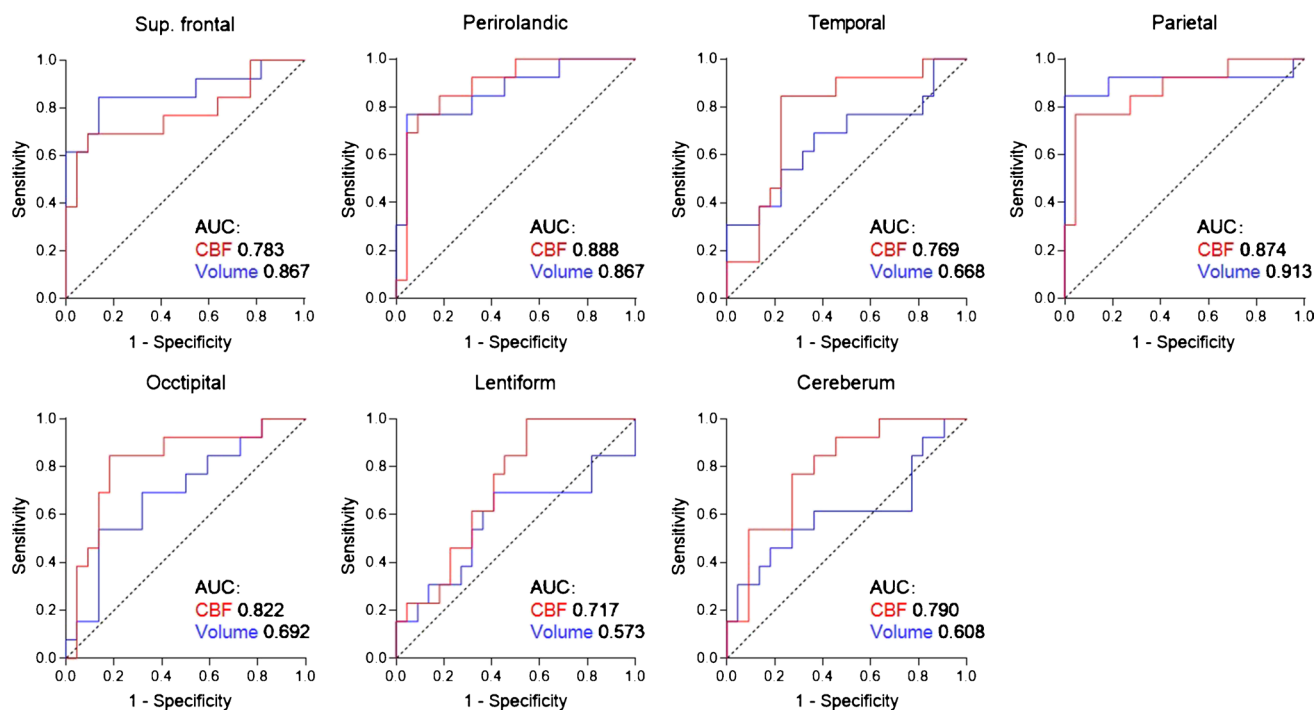


Fig. 3 Receiver operating characteristic (ROC) analysis to discriminate between patients with corticobasal syndrome (CBS) and patients with Parkinson's disease (PD) in terms of cerebral blood flow (CBF) asymmetry and cortical volume asymmetry. ROC analysis was performed in seven regions that showed significant differences between patients with CBS and those with PD either in terms of CBF asym-

metry or volume asymmetry. CBF asymmetry (red lines) showed good accuracy (area under the curve [AUC] > 0.7) in all seven regions, whereas volume asymmetry (blue lines) showed good accuracy in three regions. The AUCs of CBF asymmetry were greater than the volume asymmetry in five of the seven regions, although no significant differences were observed.

$p < 0.005$) (Fig. 4A), whereas the normalized cortical volume was lower in the perirolandic area only (2.4% vs. 2.7%, $p < 0.005$) in patients with CBS compared with patients with PD (Fig. 4B).

ROC analysis to distinguish CBS from PD showed good accuracy ($AUC > 0.7$) in these two regions (perirolandic and parietal cortices) for both analyses for the normalized CBF and volume (Fig. 4C). No significant differences in the AUCs between normalized CBF and volume were observed; however, the AUCs of the normalized CBF were greater than the normalized volume in both regions.

Discussion

In this study, we found significant CBF asymmetry in patients with CBS compared with patients with PD using ASL imaging. CBF asymmetries were observed in a wider range of brain regions than cortical volume asymmetries in patients with CBS. In addition, ROC analyses indicated that the numbers of brain regions showing good accuracy in regional asymmetries of CBF and volume (seven and three regions, respectively) were greater than the numbers showing regional decreases in the normalized CBF and volume

(two regions for both), which suggests that focusing on regional asymmetry rather than regional decrease is more effective in distinguishing between CBS and PD. Detection of asymmetrical hypoperfusion, in addition to focal atrophy, using MRI with ASL imaging has a powerful potential to aid in the diagnosis of CBS.

Similar to this study using ASL imaging, several studies with perfusion SPECT showed asymmetrical CBF reduction mainly in the frontal and parietal cortices and basal ganglia in patients with CBS or CBD compared with healthy controls [9, 12, 13, 17], patients with Alzheimer's disease [13], or patients with PD [17]. In addition, ^{18}F -FDG PET studies reported a significant asymmetrical uptake in the basal ganglia in patients with CBS compared with healthy controls [9, 14]. In the present study, significantly greater CBF asymmetries were observed in extensive cerebral cortices (perirolandic, frontal, parietal, temporal, and occipital cortices) as well as in the lentiform nucleus and cerebellar cortex in patients with CBS than in patients with PD on ASL imaging (Fig. 2A). The brain regions showing significant CBF asymmetry in this study were wider than those reported in a $^{99\text{m}}\text{Tc}$ -HMPAO SPECT study [17], which suggests that ASL imaging may be suitable in CBF asymmetry detection in patients with CBS. Moreover, in this study, ASL imaging

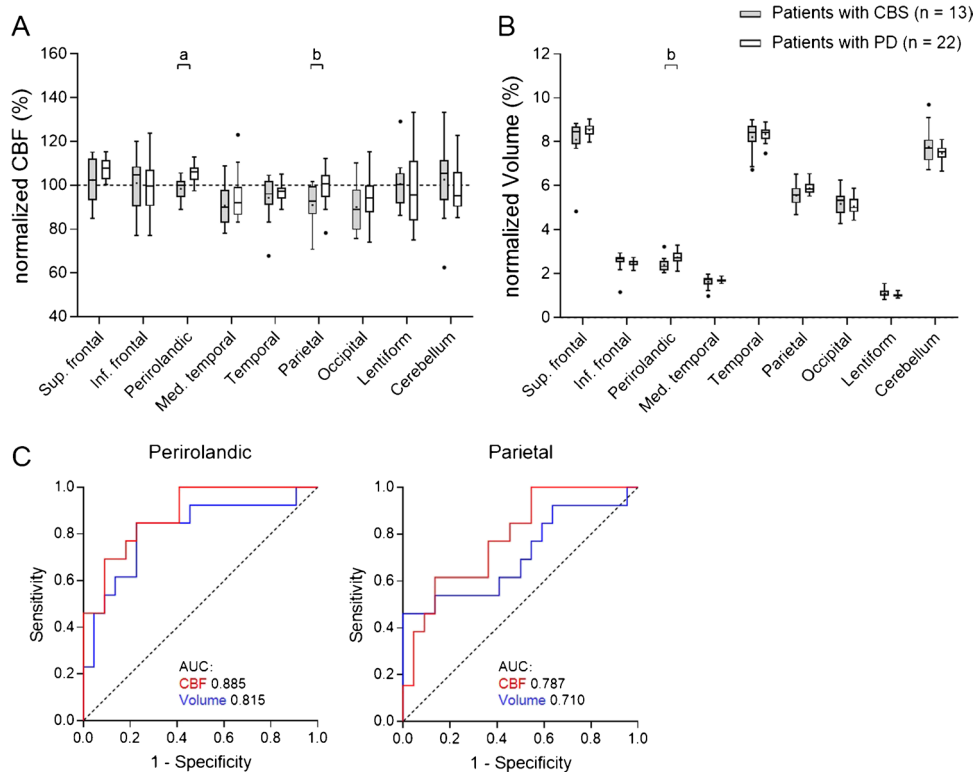


Fig. 4 Comparisons of normalized cerebral blood flow (CBF) and cortical volume in the brain regions belonging to the hemisphere contralateral to the more clinically affected side in patients with cortico-basal syndrome (CBS) and patients with Parkinson's disease (PD) **A** The normalized CBF of patients with CBS was significantly lower than that of patients with PD in two regions: perirolandic and parietal cortices. **B** The normalized cortical volume in patients with CBS

was significantly lower than that in patients with PD in one region: perirolandic area. **C** Receiver operating characteristic curve analysis to distinguish CBS from PD showed good accuracy (area under the curve [AUC] > 0.7) in these significant two regions (perirolandic and parietal cortices) in both analyses for the normalized CBF and volume (red and blue lines, respectively). p values: a < 0.001, b < 0.005

showed relatively decreased CBF in the cerebellar hemisphere ipsilateral to the more clinically affected side, probably due to crossed cerebellar diaschisis (Figs. 1 and 2A). ASL imaging detected crossed cerebellar diaschisis induced due to cerebral infarction in recent studies [30]. The assessment of crossed cerebellar diaschisis may reinforce detecting cerebral CBF asymmetry in patients with CBS on ASL imaging.

We also found that volume asymmetry showed significant differences in the perirolandic, superior frontal, and parietal cortices in patients with CBS compared with patients with PD (Fig. 2B). Several studies with volumetric MRI showed asymmetrical atrophy mainly in the frontoparietal cortex in patients with CBS compared with healthy controls, patients with Alzheimer's disease, patients with progressive supranuclear palsy, or patients with PD [8, 9, 31]. However, other recent studies reported that volume asymmetry analysis showed no significant differences in any cortical regions between patients with CBS and healthy controls [32, 33], which suggests that assessment of volume asymmetry may provide varying results. In the present study, CBF

asymmetry showed significant differences in a wider range of regions than volume asymmetry (seven regions vs. three regions, Fig. 2) in a comparison between patients with CBS and patients with PD, which indicates the relatively greater robustness of CBF asymmetry in the diagnosis of CBS.

Other studies with perfusion SPECT showed a regional CBF decrease, with no evaluation of CBF asymmetry in patients with CBS. Takaya et al. reported that hypoperfusion in the lateral frontoparietal region on perfusion SPECT was a predictor in distinguishing CBS from Lewy body disease including PD [10]. ^{18}F -FDG PET studies reported that significant hypometabolism was observed in the frontal and parietal lobes and the basal ganglia of the clinically more affected hemisphere in patients with CBS [9, 14–16]. In these studies, regional decreases in CBF or metabolism were assessed in terms of values normalized by whole-brain values [10, 11, 15–17]. Referring to these studies, we further evaluated the regional CBF decrease using the normalized CBF in the present study. As a result, patients with CBS showed significantly decreased normalized CBF in two regions (perirolandic and parietal cortices) compared with

patients with PD (Fig. 4A), which partially replicates the results of previous SPECT/PET studies [9, 12–18]. In contrast, significant CBF asymmetries were observed in seven regions (Fig. 2A), which suggests that focusing on CBF asymmetry rather than regional CBF decrease enhances the diagnostic power of ASL imaging for CBS.

This study has some limitations. First, this was a retrospective analysis with a small sample size. Second, two different post-labeling delay acquisitions (i.e., 1.5 or 2.0 s) were used for ASL imaging; however, no significant difference was observed in the mean CBF asymmetry values between the two post-labeling delay groups in patients with CBS, which suggests that the difference in post-labeling delay had little influence on CBF asymmetry. Third, MRI scans were performed at the mean disease duration from onset of approximately 3 years in both patients with CBS and those with PD. Further prospective and external validation studies utilizing a larger number of drug-naïve patients at an earlier disease stage and comparisons with radionuclide imaging are necessary to validate the diagnostic ability of the CBF asymmetry evaluation using ASL imaging, which will contribute to the implementation of this method in clinical practice. In addition, differences in the patterns of CBF asymmetry in terms of each pathological etiology of CBS should be investigated in future studies.

Conclusion

In conclusion, this study showed significant CBF asymmetry in a wider range of brain regions through the use of ASL imaging in patients with CBS compared with patients with PD. These findings suggest that ASL imaging for the detection of asymmetrical hypoperfusion has considerable clinical utility in the diagnosis of CBS.

Supplementary Information The online version contains supplementary material available at <https://doi.org/10.1007/s00234-022-02942-9>.

Funding This study was supported in part by Grant-in-Aid for Scientific Research (C) Grant Number 20K07900 from the Japan Society for the Promotion of Science (JSPS KAKENHI) (to M.I.).

Data availability Data is available on reasonable request.

Code availability Not applicable.

Declarations

Ethics approval This study was approved by the Research Ethics Committee of the University of Fukui (20170130).

Consent to participate This retrospective case–control study was approved by the Research Ethics Committee of the University of Fukui

(20170130) with a waiver of the requirement for patients' informed consent.

Consent to publication Not applicable.

Conflict of interest The authors declare that they have no conflict of interest.

References

- Dickson DW, Bergeron C, Chin SS et al (2002) Office of Rare Diseases neuropathologic criteria for corticobasal degeneration. *J Neuropathol Exp Neurol* 61:935–946. <https://doi.org/10.1093/jnen/61.11.935>
- Boeve BF, Maraganore DM, Parisi JE et al (1999) Pathologic heterogeneity in clinically diagnosed corticobasal degeneration. *Neurology* 53:795–800. <https://doi.org/10.1212/wnl.53.4.795>
- Armstrong MJ, Litvan I, Lang AE et al (2013) Criteria for the diagnosis of corticobasal degeneration. *Neurology* 80:496–503. <https://doi.org/10.1212/WNL.0b013e31827f0fd1>
- Mathew R, Bak TH, Hodges JR (2012) Diagnostic criteria for corticobasal syndrome: a comparative study. *J Neurol Neurosurg Psychiatry* 83:405–410. <https://doi.org/10.1136/jnnp-2011-300875>
- Cubo E, Martín PM, Martín-Gonzalez JA et al (2010) Motor laterality asymmetry and nonmotor symptoms in Parkinson's disease. *Mov Disord* 25:70–75. <https://doi.org/10.1002/mds.22896>
- Djalldetti R, Ziv I, Melamed E (2006) The mystery of motor asymmetry in Parkinson's disease. *Lancet Neurol* 9:796–802. [https://doi.org/10.1016/S1474-4422\(06\)70549-X](https://doi.org/10.1016/S1474-4422(06)70549-X)
- Kitagaki H, Hirono N, Ishii K, Mori E (2000) Corticobasal degeneration: evaluation of cortical atrophy by means of hemispheric surface display generated with MR images. *Radiology* 216:31–38. <https://doi.org/10.1148/radiology.216.1.r00ma0531>
- Soliveri P, Monza D, Paridi D et al (1999) Cognitive and magnetic resonance imaging aspects of corticobasal degeneration and progressive supranuclear palsy. *Neurology* 53:502–507. <https://doi.org/10.1212/wnl.53.3.502>
- Di Stasio F, Suppa A, Marsili L et al (2019) Corticobasal syndrome: neuroimaging and neurophysiological advances. *Eur J Neurol* 26:701–e52. <https://doi.org/10.1111/ene.13928>
- Takaya S, Sawamoto N, Okada T et al (2018) Differential diagnosis of parkinsonian syndromes using dopamine transporter and perfusion SPECT. *Parkinsonism Relat Disord* 47:15–21. <https://doi.org/10.1016/j.parkreldis.2017.11.333>
- Hossain AK, Murata Y, Zhang L et al (2003) Brain perfusion SPECT in patients with corticobasal degeneration: analysis using statistical parametric mapping. *Mov Disord* 18:697–703. <https://doi.org/10.1002/mds.10415>
- Okuda B, Tachibana H, Kawabata K et al (1999) Cerebral blood flow correlates of higher brain dysfunctions in corticobasal degeneration. *J Geriatr Psychiatry Neurol* 12:189–193. <https://doi.org/10.1177/089198879901200404>
- Okuda B, Tachibana H, Kawabata K et al (2001) Comparison of brain perfusion in corticobasal degeneration and Alzheimer's disease. *Dement Geriatr Cogn Disord* 12:226–231. <https://doi.org/10.1159/000051262>
- Mille E, Levin J, Brendel M et al (2017) Cerebral glucose metabolism and dopaminergic function in patients with corticobasal syndrome. *J Neuroimaging* 27:255–261. <https://doi.org/10.1111/jon.12391>
- Niethammer M, Tang CC, Feigin A et al (2014) A disease-specific metabolic brain network associated with corticobasal degeneration. *Brain* 137:3036–3046. <https://doi.org/10.1093/brain/awu256>

16. Pardini M, Huey ED, Spina S et al (2019) FDG-PET patterns associated with underlying pathology in corticobasal syndrome. *Neurology* 92:e1121–e1135. <https://doi.org/10.1212/WNL.0000000000007038>
17. Markus HS, Lees AJ, Lennox G et al (1995) Patterns of regional cerebral blood flow in corticobasal degeneration studied using HMPAO SPECT; comparison with Parkinson's disease and normal controls. *Mov Disord* 10:179–187. <https://doi.org/10.1002/mds.870100208>
18. Zhang L, Murata Y, Ishida R et al (2001) Differentiating between progressive supranuclear palsy and corticobasal degeneration by brain perfusion SPET. *Nucl Med Commun* 22:767–772. <https://doi.org/10.1097/00006231-200107000-00007>
19. Kimura H, Kado H, Koshimoto Y et al (2005) Multislice continuous arterial spin-labeled perfusion MRI in patients with chronic occlusive cerebrovascular disease: a correlative study with CO2 PET validation. *J Magn Reson Imaging* 22:189–198. <https://doi.org/10.1002/jmri.20382>
20. Detre JA, Rao H, Wang DJ et al (2012) Applications of arterial spin labeled MRI in the brain. *J Magn Reson Imaging* 35:1026–1037. <https://doi.org/10.1002/jmri.23581>
21. Melzer TR, Watts R, MacAskill MR et al (2011) Arterial spin labelling reveals an abnormal cerebral perfusion pattern in Parkinson's disease. *Brain* 134:845–855. <https://doi.org/10.1093/brain/awq377>
22. Ikawa M, Kimura H, Kitazaki Y et al (2018) Arterial spin labeling MR imaging for the clinical detection of cerebellar hypoperfusion in patients with spinocerebellar degeneration. *J Neurol Sci* 394:58–62. <https://doi.org/10.1016/j.jns.2018.09.007>
23. Ikawa M, Yoneda M, Muramatsu T et al (2013) Detection of preclinically latent hyperperfusion due to stroke-like episodes by arterial spin-labeling perfusion MRI in MELAS patients. *Mitochondrion* 13:676–680. <https://doi.org/10.1016/j.mito.2013.09.007>
24. Dashjamts T, Yoshiura T, Hiwatashi A et al (2010) Asymmetrical cerebral perfusion demonstrated by noninvasive arterial spin-labeling perfusion imaging in a patient with corticobasal degeneration. *Jpn J Radiol* 28:75–78. <https://doi.org/10.1007/s11604-009-0382-8>
25. Tomlinson CL, Stowe R, Patel S et al (2010) Systematic review of levodopa dose equivalency reporting in Parkinson's disease. *Mov Disord* 25:2649–2653. <https://doi.org/10.1002/mds.23429>
26. Hughes AJ, Daniel SE, Kilford L, Lees AJ (1992) Accuracy of clinical diagnosis of idiopathic Parkinson's disease: a clinicopathological study of 100 cases. *J Neurol Neurosurg Psychiatry* 55:181–184. <https://doi.org/10.1136/jnnp.55.3.181>
27. Dai W, Garcia D, de Bazelaire C, Alsop DC (2008) Continuous flow-driven inversion for arterial spin labeling using pulsed radio frequency and gradient fields. *Magn Reson Med* 60:1488–97. <https://doi.org/10.1002/mrm.21790>
28. Hammers A, Allom R, Koeppe MJ et al (2003) Three-dimensional maximum probability atlas of the human brain, with particular reference to the temporal lobe. *Hum Brain Mapp* 19:224–247. <https://doi.org/10.1002/hbm.10123>
29. Gousias IS, Rueckert D, Heckemann RA et al (2008) Automatic segmentation of brain MRIs of 2-year-olds into 83 regions of interest. *Neuroimage* 40:672–684. <https://doi.org/10.1016/j.neuroimage.2007.11.034>
30. Chen S, Guan M, Lian HJ et al (2014) Crossed cerebellar diaschisis detected by arterial spin-labeled perfusion magnetic resonance imaging in subacute ischemic stroke. *J Stroke Cerebrovasc Dis* 23:2378–2383. <https://doi.org/10.1016/j.jstrokecerebrovasdis.2014.05.009>
31. Hauser RA, Murtaugh FR, Akhter K et al (1996) Magnetic resonance imaging of corticobasal degeneration. *J Neuroimaging* 6:222–226. <https://doi.org/10.1111/jon199664222>
32. Upadhyay N, Suppa A, Piattella MC et al (2016) Gray and white matter structural changes in corticobasal syndrome. *Neurobiol Aging* 37:82–90. <https://doi.org/10.1016/j.neurobiolaging.2015.10.011>
33. Gröschel K, Hauser TK, Luft A et al (2004) Magnetic resonance imaging-based volumetry differentiates progressive supranuclear palsy from corticobasal degeneration. *Neuroimage* 21:714–724. <https://doi.org/10.1016/j.neuroimage.2003.09.070>

Publisher's note Springer Nature remains neutral with regard to jurisdictional claims in published maps and institutional affiliations.